

Characterization of carbonaceous aerosols outflow from India and Arabia: Biomass/biofuel burning and fossil fuel combustion

S. A. Guazzotti,¹ D. T. Suess,² K. R. Coffee,^{2,3} P. K. Quinn,⁴ T. S. Bates,⁴ A. Wisthaler,⁵ A. Hansel,⁵ W. P. Ball,⁶ R. R. Dickerson,⁷ C. Neusüß,^{8,9} P. J. Crutzen,^{10,11} and K. A. Prather¹

Received 2 December 2002; revised 25 February 2003; accepted 11 March 2003; published 15 August 2003.

[1] A major objective of the Indian Ocean Experiment (INDOEX) involves the characterization of the extent and chemical composition of pollution outflow from the Indian Subcontinent during the winter monsoon. During this season, low-level flow from the continent transports pollutants over the Indian Ocean toward the Intertropical Convergence Zone (ITCZ). Traditional standardized aerosol particle chemical analysis, together with real-time single particle and fast-response gas-phase measurements provided characterization of the sampled aerosol chemical properties. The gas- and particle-phase chemical compositions of encountered air parcels changed according to their geographic origin, which was traced by back trajectory analysis. The temporal evolutions of acetonitrile, a long-lived specific tracer for biomass/biofuel burning, number concentration of submicrometer carbon-containing particles with potassium (indicative of combustion sources), and mass concentration of submicrometer non-sea-salt (nss) potassium are compared. High correlation coefficients ($0.84 < r^2 < 0.92$) are determined for these comparisons indicating that most likely the majority of the species evolve from the same, related, or proximate sources. Aerosol and trace gas measurements provide evidence that emissions from fossil fuel and biomass/biofuel burning are subject to long-range transport, thereby contributing to anthropogenic pollution even in areas downwind of South Asia. Specifically, high concentrations of submicrometer nss potassium, carbon-containing particles with potassium, and acetonitrile are observed in air masses advected from the Indian subcontinent, indicating a strong impact of biomass/biofuel burning in India during the sampling periods (74 (± 9)% biomass/biofuel contribution to submicrometer carbonaceous aerosol). In contrast, lower values for these same species were measured in air masses from the Arabian Peninsula, where dominance of fossil fuel combustion is suggested by results from single-particle analysis and supported by results from gas-phase measurements (63 (± 9)% fossil fuel contribution to submicrometer carbonaceous aerosol). Results presented here demonstrate the importance of simultaneous, detailed gas- and particle-phase measurements of related species when evaluating possible source contributions to aerosols in different regions of the world. *INDEX TERMS*: 0305 Atmospheric Composition and Structure: Aerosols and particles (0345, 4801); 0345 Atmospheric Composition and Structure: Pollution—urban and regional (0305); 0394 Atmospheric Composition and Structure: Instruments and techniques; *KEYWORDS*: INDOEX, aerosol chemical characterization, biomass burning, fossil fuel combustion

Citation: Guazzotti, S. A., et al., Characterization of carbonaceous aerosols outflow from India and Arabia: Biomass/biofuel burning and fossil fuel combustion, *J. Geophys. Res.*, 108(D15), 4485, doi:10.1029/2002JD003277, 2003.

¹Department of Chemistry and Biochemistry, University of California, San Diego, California, USA.

²Department of Chemistry, University of California, Riverside, California, USA.

³Now at Lawrence Livermore National Laboratory, Livermore, California, USA.

⁴Pacific Marine Environmental Laboratory, NOAA, Seattle, Washington, USA.

⁵Institut für Ionenphysik, University of Innsbruck, Innsbruck, Austria.

⁶Department of Chemistry, University of Maryland, College Park, Maryland, USA.

⁷Department of Meteorology and Department of Chemistry, University of Maryland, College Park, Maryland, USA.

⁸Institut für Troposphärenforschung, Leipzig, Germany.

⁹Now at Bruker Daltonik, Leipzig, Germany.

¹⁰Max-Planck Institute for Chemistry, Mainz, Germany.

¹¹Also at Scripps Institution of Oceanography, University of California, San Diego, California, USA.

1. Introduction

[2] Anthropogenic activities influence the chemical composition of the atmospheric aerosol, therefore affecting climate, visibility, and human health. Knowledge of the chemical composition and size distribution of aerosol particles, as well as the chemical characteristics and mixing ratios of different species present in the gas phase, is essential for understanding atmospheric processing that affects the composition of aerosols as well as for identification of their sources. During the past few years, increases in the concentration of atmospheric aerosols due to anthropogenic activities have been the focus of many studies [e.g., IPCC, 1996; Schwartz, 1996; Schwartz and Andreae, 1996]. Almost five-fold increases in concentrations of certain species (e.g., nitrates, sulfates) have been indicated for regions downwind of the Indian Subcontinent in the last twenty years [Ball et al., 2003].

[3] Combustion processes such as biomass/biofuel burning and fossil fuel combustion are significant sources of anthropogenic aerosol particles and gases [e.g., Andreae and Crutzen, 1997; Yamasoe et al., 2000; Andreae and Merlet, 2001]. Particles emitted from these sources can affect the radiation balance due to their ability to reflect and absorb solar radiation (direct effect) and act as cloud condensation nuclei, therefore affecting cloud properties (indirect effect) [e.g., Twomey, 1977; Coakley and Cess, 1985; Desalmand et al., 1985; Hallet et al., 1989; Crutzen and Andreae, 1990; Andreae, 1991; Cachier and Ducret, 1991; Charlson et al., 1991; Kuhlbusch et al., 1996; Rosenfeld, 2000]. Emissions from biomass/biofuel burning and other combustion sources which emit black carbon can significantly heat the atmosphere [e.g., Crutzen and Andreae, 1990; Penner et al., 1992, 1993; Haywood and Shine, 1995, 1997; Iversen and Tarrason, 1995; Cooke and Wilson, 1996; Haywood et al., 1997; Haywood and Boucher, 2000; Iversen et al., 1998; Podgorny et al., 2000; Jacobson, 2001; Ramanathan et al., 2001]. Penner et al. [1992] have shown that the direct and indirect effects of smoke aerosols arising from biomass burning could be of comparable significance.

[4] Biomass fuels account for approximately 14% of the world's energy consumption [Hall et al., 1992], with much higher values being reported for developing countries. In India, biomass/biofuel burning (including wood, agricultural residues, and dung-cakes used as fuel) is considered to be a major source of energy [Ravindranath and Hall, 1995] and a considerable source of pollution [Hall et al., 1994; Dickerson et al., 2002]. High overall increases in the consumption of petroleum, biofuels, and coal have been reported for the Indian subcontinent. Up to 45% of global emissions of black carbon have been attributed to biomass/biofuel burning [e.g., Kuhlbusch et al., 1996] with emissions from India [1990] estimated to account for $0.45\text{--}1\text{ Tg yr}^{-1}$ [Reddy and Venkataraman, 2000]. Direct observations show that the emissions could be as high as 3 Tg yr^{-1} [Dickerson et al., 2002].

[5] The Indian Ocean Experiment, INDOEX, was an integrated field campaign which had as a primary goal evaluating the significance of the direct and indirect effects of continental aerosols [Ramanathan et al.,

1995, 1996, 2001; Satheesh et al., 1999; Mitra, 1999]. Characterization of the extent and chemical composition of pollution outflow from the Indian subcontinent and evaluation of the significance of long-range transport of continental aerosols to remote regions in the Indian Ocean were of particular interest [Ramanathan et al., 1995, 1996; 2001]. Ramanathan et al. [2001] have highlighted, from results obtained during the INDOEX campaign, the impact of the Indo-Asian haze on global climate. The biomass/biofuel and fossil fuel contributions to this Indo-Asian haze have been reported to be under debate [UNEP, 2002]. The INDOEX intensive field phase (INDOEX-IFP) was carried out in February and March 1999, during the winter monsoon (NE-monsoon), when low level flow from the continent transports pollutants over the Indian Ocean toward the Intertropical Convergence Zone (ITCZ), where pristine southern hemisphere air masses meet with contrasting polluted continental air masses from the northern hemisphere. During the IFP, the contribution of anthropogenic aerosols to the total loading has been estimated to be as high as 80% over most of the sampled south Asian region and Northern Indian Ocean [Ramanathan et al., 2001].

[6] Several measurements were performed during the campaign on different platforms (for a detailed description see Lelieveld et al. [2001] and Ramanathan et al. [2001]). Results from aerosol particle and gas-phase measurements carried out during leg 2 of the INDOEX cruise on board of the NOAA Research Vessel (R/V) Ronald H. Brown are presented here. Chemical characterization of sampled aerosol particles included mass concentrations of submicrometer non-sea-salt (nss) potassium (K^+), nss sulfate, black carbon (BC), organic carbon (OC), and number concentration of submicrometer carbon-containing particles with K^+ . In the gas-phase, the volume mixing ratio of acetonitrile (methyl cyanide, CH_3CN) was measured. During the sampling period, the ITCZ was mostly located between the equator and 12°S [Ramanathan et al., 2001; Ball et al., 2003]. Detailed information on the R/V Ronald H. Brown cruise during INDOEX can be found in Ball et al. [2003]. The capability descriptions for this vessel are presented in Parsons and Dickerson [1999].

[7] Acetonitrile is regarded as a relatively long-lived, selective tracer for biomass/biofuel burning [Lobert et al., 1990; Bange and Williams, 2000], predominantly emitted by smoldering biomass fires [Lobert et al., 1990; Holzinger et al., 1999]. In the particle phase, black carbon BC in the submicrometer size range is used as a good general tracer for incomplete combustion from fossil fuel and biomass burning [e.g., Cachier et al., 1989], while nss K^+ is considered to be a good indicator for biomass/biofuel burning in submicrometer particles [e.g., Andreae, 1983; Cachier et al., 1991; Gaudichet et al., 1995; Andreae et al., 1996]. In particular, the relative contributions from biomass and fossil fuel emissions can be evaluated from the ratio between submicrometer nss K^+ and BC [Andreae, 1983]. From single particle measurements, submicrometer soot particles containing K^+ have been indicated as possible tracers for biomass/biofuel burning [Gaudichet et al., 1995]. Single-particle results obtained during INDOEX and combustion

source characterization experiments provide an indication of probable sources of the carbonaceous aerosol.

2. Experimental Setup

[8] The data presented herein were obtained from 4 March 1999 (Day of Year, DOY 63) until 23 March 1999 (DOY 82) during leg 2 of the NOAA R/V Ronald H. Brown 1999 INDOEX cruise. The cruise started in Male', the capital of the Republic of the Maldives, proceeding along the west coast of India and turning south on 11 March (DOY 70). The southern-most point during leg 2 (13°S) was reached on 19 March (DOY 78).

2.1. Submicrometer Non-Sea-Salt (nss) Potassium and nss Sulfate Mass Concentration

[9] Two independent research groups on board the NOAA R/V Ronald H. Brown, namely NOAA, Pacific Marine Environmental Laboratory (PMEL), Seattle, Washington and Department of Meteorology, University of Maryland, College Park (UMD), measured submicrometer nss K^+ and nss sulfate mass concentrations. PMEL used two-stage multijet cascade impactors [Berner *et al.*, 1979] sampling air at 55% RH to determine the submicrometer ($D_{50,aero} < 1.1 \mu\text{m}$) concentration of sulfate and K^+ . The impaction stage at the inlet of the impactor was coated with silicone grease to prevent the bounce of larger particles onto the downstream stages. A Millipore Fluoropore filter (1.0 μm pore size) was used for the submicrometer collection substrate. Filters were wetted with 1 mL of spectral grade methanol. An additional 5 mL aliquot of distilled deionized water was added to the solution and the substrates were extracted by sonicating for 30 min. The extracts were analyzed by ion chromatography [Quinn *et al.*, 1998]. Blank levels were determined by loading an impactor with substrates but not drawing any air through them. In the case of UMD, two high volume Sierra impactors, one cascade and one bulk, were used to collect aerosol samples [Howell *et al.*, 1998]. The cascade impactor consisted of five stages that segregated the total particular material into six size fractions. Slotted Whatman 41 filters were used as the impaction surfaces. The mean aerodynamic diameter for the stages reported here were 0.74, 0.48, and 0.24 μm [Pszenny, 1992]. A backup filter collected particles under 0.24 μm . The bulk impactor consisted of a 20 cm by 25 cm Whatman filter. After sampling, filters were placed into individual polyethylene bags and refrigerated. On alternate days, samples were analyzed on the ship as described by Quinn *et al.* [1998]. The remaining samples were analyzed upon return to the United States using the same method. Results presented here for UMD correspond to particles with mean aerodynamic diameters smaller than 0.74 μm . In both cases, nss K^+ concentrations were calculated from Na^+ concentrations and the ratio of K^+ to sodium in seawater. Similarly, nss sulfate concentrations were evaluated from the measured sulfate concentrations and the corresponding sulfate-to-sodium ratio in seawater.

2.2. Black Carbon/Organic Carbon (BC/OC) Mass Concentration

[10] Submicrometer particles in the range $0.18 < D_p < 1.1 \mu\text{m}$ were collected using a three-stage multijet cascade impactor [Berner *et al.*, 1979] as described in Neusüß *et al.*

[2002a]. For the determination of BC/OC, a thermographic method (Ströhlein C-mat 5500 carbon analyzer) was operated at a temperature of 590°C to volatilize the OC fraction within 8 min under nitrogen. The BC fraction of aerosol particle samples was determined by subsequent combustion at 650°C in an oxygen atmosphere. For a detailed explanation of the method used for the evaluation of BC/OC during the INDOEX cruise, as carried out by the research group from the Institute for Tropospheric Research, Germany, refer to Neusüß *et al.* [2002a]. It is important to mention that, although there are several methods to determine separately OC and BC, there is no technique that is commonly accepted. Methods currently in use include extraction and thermodesorption methods, with the latter method having the advantage of being less labor intensive. Comparison experiments among the different techniques for BC/OC yield sufficient comparability of total carbon (TC) values but a wide spread in results of OC and BC determinations. [Cadle and Mulawa, 1990; Countess, 1990; Shah and Rau, 1991; Schmid *et al.*, 2001]. The method used for the determination described here typically leads to higher BC/OC ratios compared to related techniques (i.e., provides a lower limit for OC and an upper limit for BC), but it has the advantage of lacking positive artifacts. Quartz fiber filter sampling for the evaluation of OC show typically high positive sampling artifacts due to the absorption of volatile organic species [e.g., Turpin *et al.*, 1994]. Such positive artifacts are expected to be low for impactor sampling, since foils have a much smaller surface than the fiber filters. Better impactor sampling efficiencies, compared to filter sampling for semivolatile particles, have been observed by Wang and John [1988] and Neusüß *et al.* [2002b]. This might be due to reduced aeration of collected particles on the impactor substrates compared to filter substrates, possibly over compensating losses due to the pressure drop in the impactor. However, the low pressure could lead to losses of semivolatile organic compounds during sampling, mainly for the submicrometer particle fraction. The method has not been corrected for any sampling artifacts.

2.3. Single-Particle Analysis

[11] Data on individual particle size and chemical composition were obtained by the research group from the University of California, San Diego using a transportable aerosol time-of-flight mass spectrometer (ATOFMS) as described in the literature [e.g., Prather *et al.*, 1994; Noble and Prather, 1996; Gard *et al.*, 1997]. In these instruments, the transit times for particles travelling between two scattering lasers are measured, recorded, and correlated with the individual particle aerodynamic diameters after proper instrument calibration. Chemical information for each detected particle is obtained from positive and negative ion time-of-flight mass spectra acquired in the instrument, and correlated with the aerodynamic diameter measured for each particle. Detected particles are classified into exclusive chemical categories from the mass spectral information obtained for each individual particle. Particle number concentrations for different particle classes are then evaluated by carrying out scaling procedures to account for differences in particle transmission into the ATOFMS [e.g., Hughes *et al.*, 1999; Allen *et al.*, 2000]. In this particular case, ATOFMS data were scaled by comparison with

number concentration data obtained with other shipboard particle sizing instrumentation (i.e., Optical Particle Counter (OPC), and a Scanning Mobility Particle Sizer (SMPS)) [Wenzel *et al.*, 2003]. A more detailed explanation on the instrumental set-up used during the campaign as well as of the types of particles observed during INDOEX is presented by Guazzotti *et al.* [2001]. All the single particle results presented herein correspond to particles with aerodynamic diameters between 0.3 and 1.0 μm .

2.4. Fast-Response Acetonitrile Measurements by PTR-MS

[12] Fast-response measurements of acetonitrile were performed using Proton-Transfer-Reaction Mass Spectrometry (PTR-MS) by the research group from Institut für Ionenphysik, University of Innsbruck, Austria [Hansel *et al.*, 1995; Lindinger *et al.*, 1998]. PTR-MS is a chemical ionization mass spectrometry technique based on proton transfer reactions with H_3O^+ ions for on-line measurements of organic trace gases in air. PTR-MS measurements during INDOEX-IFP have been described in detail by Sprung *et al.* [2001] and Wisthaler *et al.* [2002], thus only the essential points are outlined here. Ambient air was continuously sampled through a Teflon[®] PFA tube (length: 50 m; OD: 6.4 mm) from the top of the Ronald H. Brown bow tower (28m above sea surface) and led into the PTR-MS instrument. Chemical ionization of acetonitrile (producing the CH_3CNH^+ ion at mass-to-charge ratio (m/z) 42) was achieved using proton-transfer-reactions with primary H_3O^+ ions in a flow drift tube. Primary and product ions were mass analyzed in a quadrupole mass spectrometer and detected by a secondary electron multiplier/pulse counting system. The sensitivity for acetonitrile was calculated following the procedure outlined in detail by Sprung *et al.* [2001]. The instrumental background was determined by passing the ambient air through a heated platinum catalyst (350°C) scrubber. Accuracy for the acetonitrile measurements of $\pm 30\%$ was inferred from intercomparison measurements described by Sprung *et al.* [2001].

2.5. Aerosol Absorption Coefficient

[13] The absorption coefficients for submicrometer aerosol particles were measured at 55% RH by monitoring the change in transmission through a filter with a Particle Soot Absorption Photometer (PSAP, Radiance Research). Measured values were corrected for a scattering artifact, the deposit spot size, the PSAP flow rate, and the manufacturer's calibration as per Bond *et al.* [1999]. Values are reported at 0°C, 1013 mbar, and 550 nm. Sources of uncertainty in the PSAP measurement include noise, drift, correction for the manufacturer's calibration, and correction for the scattering artifact [Anderson *et al.*, 1999]. A quadrature sum of these errors yields absolute uncertainties of 0.38 and 2.8 Mm^{-1} for absorption coefficients equal to 0.68 and 13 M m^{-1} , respectively. These measurements were carried out by PMEL.

3. Results and Discussion

3.1. Carbon-Containing Particles With Potassium

[14] During INDOEX, the majority of detected particles with aerodynamic diameters between 0.3 and 1.0 μm were classified as carbon-containing particles by ATOFMS single

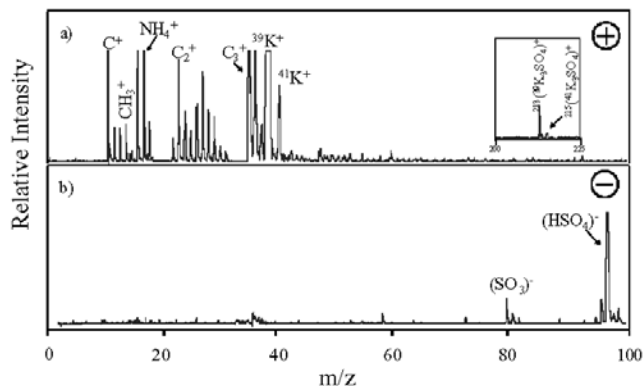


Figure 1. (a) Positive and (b) negative ion mass spectra of a carbon-containing particle with potassium acquired during INDOEX. Peak identifications correspond to the most probable assignments for each particular m/z ratio.

particle analysis [Guazzotti *et al.*, 2001]. Between 20 and 73% of the submicrometer carbon-containing particles detected with the ATOFMS contained K^+ as well, depending on the location considered [Guazzotti *et al.*, 2001]. The presence of K^+ in submicrometer carbon-containing particles has been described to be an indicator of biomass/biofuel combustion [e.g., Andreae, 1983; Gaudichet *et al.*, 1995; Andreae *et al.*, 1996; Andreae and Crutzen, 1997; Silva *et al.*, 1999; Yamasoe *et al.*, 2000] and/or coal combustion (D. T. Suess *et al.*, manuscript in preparation). Potassium is not detected in emissions from light duty gasoline powered vehicles currently in use in the U.S. (mostly four-stroke engines) [Silva and Prather, 1997]. Also, submicrometer soot particles emitted from diesel engine exhaust have been reported to contain no detectable amounts of potassium [Gaudichet *et al.*, 1995]. However, no ATOFMS data are available for the vehicle fleet currently in use on the Indian Subcontinent (mostly two-stroke engines [UNEP, 1999] for which emission data are also lacking [Dickerson *et al.*, 2002]).

[15] ATOFMS positive and negative ion mass spectra representative of a typical carbon-containing particle with K^+ are presented in Figure 1. In the positive ion mass spectrum (Figure 1a), C^+ , $(\text{CH}_3)^+$, $(\text{C}_2)^+$, $(\text{C}_2\text{H}_3)^+$, $(\text{C}_3)^+$, $(\text{C}_3\text{H})^+$ ions are observed, together with other ion peaks associated with hydrocarbon envelopes $(\text{C}_n\text{H}_m)^+$. Peaks at mass-to-charge ratios (m/z) 39 ($^{39}\text{K}^+$) and 41 ($^{41}\text{K}^+$) indicate the presence of K^+ . The peak at m/z 18 is assigned to NH_4^+ . Peaks at m/z 213 and 215 are assigned to potassium sulfate ions $^{213}(\text{K}_3\text{SO}_4)^+$ and $^{215}(\text{K}_3\text{SO}_4)^+$, respectively. The peak at m/z 97 is assigned to HSO_4^- (Figure 1b). The presence of sulfate on carbonaceous particles can result from direct emission by combustion sources, coagulation, cloud processing, and/or condensation and oxidation of sulfur dioxide on particles. Sulfate was usually observed in the carbonaceous particles detected during INDOEX (average sulfate associations for particles with aerodynamic diameters between 0.3 and 1.0 μm were determined to be 75% for carbon-containing particles with K^+) [Guazzotti *et al.*, 2001]. In the negative ion mass spectra of these particles, carbon ion clusters, such as C^- , $(\text{C}_2)^-$, $(\text{C}_3)^-$, and $(\text{C}_4)^-$, were periodically observed.

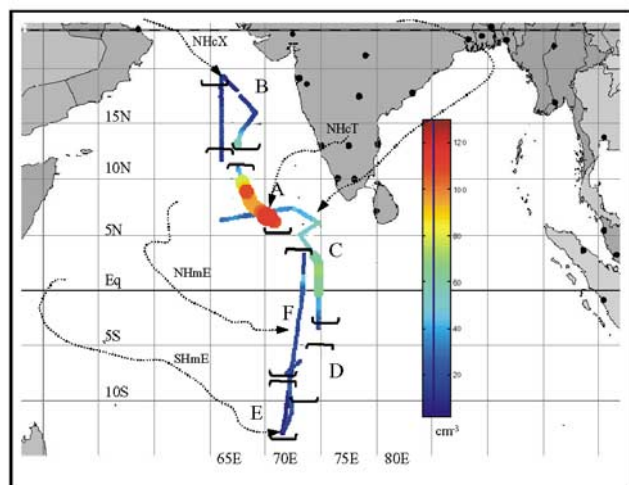


Figure 2. Spatial distribution of carbon-containing particles with potassium (aerodynamic diameter between 0.3 and 1.0 μm) along the cruise track of leg 2 of the NOAA R/V Ronald H. Brown. Regions A–F along the cruise track, impacted by different air mass source regions, are indicated together with typical 7-day back trajectories (ending at 950 hPa) indicative of the flow regimes described in the text.

[16] Particles are classified as carbon-containing with K^+ by carrying out exclusive searches in a Matlab[®] based database where threshold values (ion area, relative ion area, mass-to-charge ratios, etc.) for specific ions are specified. In this study, a relative area of greater than 10% for the peak at m/z 39 ($^{39}\text{K}^+$) is used for identification. The presence of a combination of at least two peaks at mass-to-charge ratios 12 (C^+), 36 (C_3^+), 48 (C_4^+), 60 (C_5^+), and 72 (C_6^+) with areas higher than 40 (arbitrary units) is required for these particles to be classified as carbon-containing with K^+ . Particles cannot be classified into more than one class (such as sea salt, dust, carbon-containing with no K^+ , etc.), therefore making the chemical classes exclusive. Once the particles are classified, their temporal evolution is evaluated and compared with results obtained with other techniques. In this classification scheme, no requirements are imposed in terms of ions that indicate the presence of sulfate and/or chloride, although one or both ions were observed in almost all of the mass spectra of the carbon-containing particles with K^+ . It has been previously shown that the presence of chloride and/or sulfate in combustion related particles depends on the temperature of formation of the particles as well as their aging process [e.g., Gaudichet et al., 1995; Ruellan et al., 1999; Liu et al., 2000]. For example, in the case of particles produced from biomass burning, Gaudichet et al. [1995] have indicated that near the emission sources more chlorine occurs in the observed soot particles than those collected farther downwind from the sources, indicating the evolution from KCl to K_2SO_4 .

[17] Figure 2 shows the spatial distribution of carbon-containing particles with K^+ along the cruise track for leg 2 of the INDOEX cruise. The cruise track was divided into 6 regions based on the geographical origin of the sampled air masses. These regions follow the classification of Ball et al. [2003] and are based on back trajectory analysis [Quinn et al., 2002]. The back trajectories were calculated using the

Hybrid Single-Particle Lagrangian Integrated Trajectory model (HY-SPLIT 4) [Draxler, 1991; Draxler and Hess, 1998]. The six regimes encountered during leg 2 of the cruise, as indicated in Figure 2, are (A) Northern Hemisphere Continental Tropical (NHcT) (Indian Subcontinent air mass), (B) Northern Hemisphere Continental Extratropical (NHcX) (Arabian Peninsula air mass), (C) Mixed Northern Hemisphere Continental (mixed NHc) (Arabian/Indian Subcontinent air mass), (D) Northern Hemisphere Maritime Equatorial (NHmE) (Northern Indian Ocean air mass), (E) Southern Hemisphere Maritime Equatorial (SHmE) (Southern Indian Ocean air mass), and (F) Northern Hemisphere Maritime Equatorial (Northern Indian Ocean air mass). Detailed explanations of the regimes described above are presented by Ball et al. [2003] and Mühle et al. [2002]. An overview of the regional meteorological circumstances during INDOEX-IFP is given by Verver et al. [2001].

[18] The number concentration of carbon-containing particles with K^+ was highest for the time period DOY 65.07–67.54, which corresponds to Region A (moving from 6.1°N 71.3°E to 13.8°N 68.6°E). Region A was the most polluted based on the overall particle loading, aerosol optical depth, and trace gases mixing ratios [de Laat et al., 2001; Guazzotti et al., 2001; Ball et al., 2003; Mühle et al., 2002; Neusüß et al., 2002a; Quinn et al., 2002; Wisthaler et al., 2002]. In the northernmost region, Region B (DOY 68.08–69.85, moving from 15.1°N 69.4°E to 19.0°N 67.1°E), a decrease in the number concentration of carbon-containing particles with K^+ was observed. During this period, the winds were mostly from the north. Back trajectories show general subsidence starting at 200–400 mbar above the Arabian Peninsula six days upwind subsiding to 950 mbar just one or two days before reaching the R/V Ronald H. Brown [Quinn et al., 2002]. In this region, an increase in the number concentration of dust particles [Guazzotti et al., 2001] and in the mass concentration of nss Ca^{2+} and ash (noncombustible mineral dust) [Ball et al., 2003] was observed, indicating that the overall aerosol chemical composition had an influence from dust particles being transported from the Middle East (K. R. Coffee et al., manuscript in preparation). In the southernmost locations, a decrease in the number concentration of carbon-containing particles with K^+ was observed (Region E, DOY 78.59–79.50). During that time period, the sampled air had no continental influence for 6 to 7 days, with the ITCZ located at approximately 12°S [Ball et al., 2003].

3.2. Comparison of Single Particle Results to Other Particle- and Gas-Phase Data sets

[19] In Figure 3, the observed temporal evolution of the number concentration of carbon-containing particles with K^+ is compared with the corresponding evolution of the mass concentration of submicrometer nss K^+ measured by two different research groups (PMEL and UMD) and the gas-phase acetonitrile mixing ratio. The same general trends are observed for both the particle- and gas-phase. The highest number concentration of carbon-containing particles with K^+ , mass concentration of submicrometer nss K^+ , and acetonitrile mixing ratio occurred during the time period DOY 65.07–67.54, Region A (average values 62 (± 16) cm^{-3} , 0.35 (± 0.14) $\mu\text{g m}^{-3}$, and 276 (± 9) pptv respectively). The

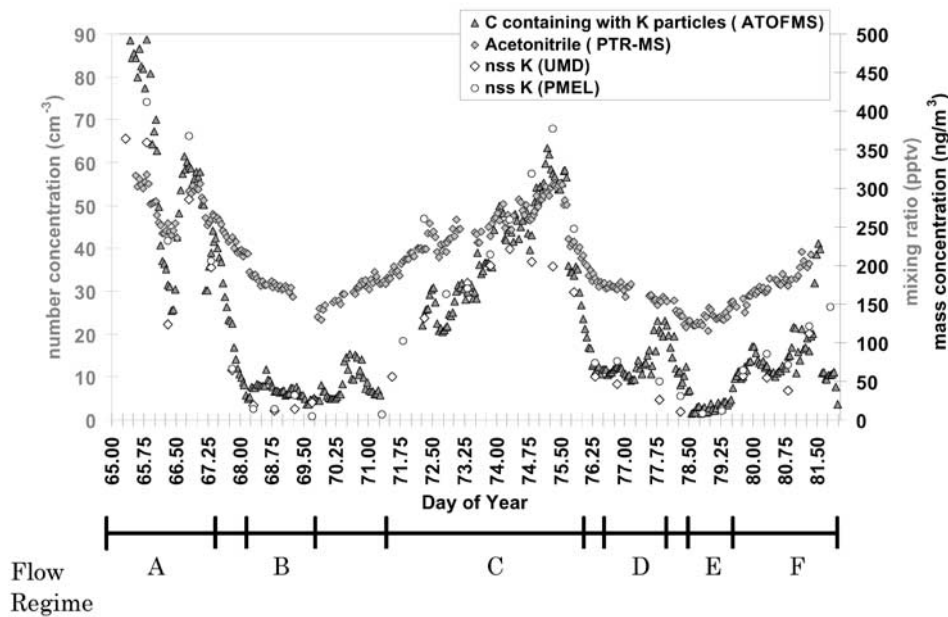


Figure 3. Temporal evolutions of submicrometer nss potassium mass concentration (PMEL and UMD), number concentration of carbon-containing particles with potassium, and acetonitrile mixing ratio observed during leg 2 of the INDOEX cruise.

average values for the different regions are summarized in Table 1. In the northernmost locations (Region B, DOY 68.08–69.85), a decrease is evident in all values (average values $7 (\pm 2) \text{ cm}^{-3}$, $0.017 (\pm 0.012) \mu\text{g}/\text{m}^3$, and $178 (\pm 18) \text{ pptv}$) (see Table 1). As indicated, during this time the winds were mostly from the North, with air masses having an influence from the Arabian Peninsula. In the southernmost locations, when the sampled air mass had no continental influence for at least 6 to 7 days, decreases in the number concentrations of all species were observed. Average concentrations decreased to their minimum observed values for the time period DOY 78.59–79.50 (see Table 1). Average number concentrations for particles with optical diameters between 0.3 and $1.0 \mu\text{m}$, as determined by an Optical Particle Counter (OPC) (Particle Measuring Systems, Inc.) aboard the R/V Ronald H. Brown, are also presented in Table 1 for comparison purposes. As shown in the Table, the same general trends discussed above apply to the overall number concentration of submicrometer particles. When compared to the values determined with the OPC, carbon-containing particles with K^+ represented 63 and 58% of the submicrometer particles in Regions A and B, respectively. Aerosol number size distributions measured during the research cruise using a differential mobility particle sizer (DMPS) and an aerodynamic particle sizer (APS) are presented in Bates *et al.* [2002].

[20] Results from comparisons between submicrometer nss K^+ mass concentration measured by two different research groups (PMEL and UMD) show a high correlation factor between results ($r^2 = 0.91$), indicating that no particular contamination or interference was experienced. The mass concentration values reported by UMD are consistently lower than those from PMEL due to the different size-cuts used for the corresponding evaluations ($0.74 \mu\text{m}$ and $1.0 \mu\text{m}$ respectively, see section 2.1). Mass concentration values of

submicrometer nss K^+ are highly correlated with the number concentration of carbon-containing particles with K^+ detected with ATOFMS ($r^2 = 0.92$). The high correlation indicates that most of the submicrometer nss K^+ was associated with carbonaceous material. A high correlation factor ($r^2 = 0.84$) is found between the number concentrations of carbon-containing particles with K^+ and gas-phase acetonitrile mixing ratios. Such good agreement is unexpected since deposition effects that govern the particle-phase would usually prevent the observation of a high correlation between gas- and particle-phase measurements of associated or related species. In particular, removal of particles from the lower troposphere due to precipitation has to be taken into consideration when comparing these results. Most of the data presented here were collected during time periods when no precipitation events occurred at the sampling site. Rain was encountered only near the ITCZ, where overall concentrations were low, and only a limited number of rain events were experienced during the air mass transport from the source. Lack of rain is typically experienced during the winter monsoon season [e.g., Rasch *et al.*, 2001]. The high correlation obtained for the number concentrations of submicrometer carbon-containing particles with K^+ and the mixing ratios of acetonitrile most likely indicates that both arise from the same, related, or proximate sources. The correlation between the number concentration of carbon-containing particles with K^+ and the measured submicrometer absorption coefficient is evaluated as well. The strong correlation ($r^2 = 0.92$) indicates that submicrometer carbon-containing particles with K^+ are most likely the major contributors to the observed absorption. Neusüß *et al.* [2002a] arrived at similar conclusions from absorption and BC mass concentration measurements. Satheesh *et al.* [1999] suggested that BC from combustion sources is responsible for the strong absorption observed in this area.

Table 1. Average Values Obtained for Different Air Masses and Flow Regimes^a

Region	Day of Year	Flow Regime ^b	Air Mass Type ^c	Absorption		Acetonitrile, pptv	CcwK ₃ ^e cm ⁻³	Nss K ^{+d} μg m ⁻³	Nss K ⁺ /BC	Nss SO ₄ ²⁻ /BC	BC/OC	Number Concentration, cm ⁻³
				Coefficient, M m ⁻¹	7 (3)							
A	65.07–67.54	NHcT	Indian Subcontinent	11.4 (4.3)	0.35 (0.14)	276 (9)	62 (16)	0.4 (0.2)	7 (3)	1.5 (0.6)	99 (25)	
B	68.08–69.85	NHcX	Arabian Peninsula	0.97 (0.18)	0.017 (0.012)	178 (18)	7 (2)	0.18 ^g	11.8 ^g	0.22 ^g	12 (3)	
C	71.57–76.04	Mixed NHc	Arabian/Indian Subcontinent	6.4 (2.4)	0.24 (0.09)	248 (31)	39 (12)	0.5 (0.2)	9 (4)	1.2 (0.5)	55 (16)	
D	76.59–78.04	NHmE	Northern Indian Ocean	2.0 (0.4)	0.063 (0.018)	165 (9)	14 (4)	0.62 (0.04)	11 (4)	1.59 (0.02)	23 (6)	
E	78.59–79.50	SHmE	Southern Indian Ocean	0.50 (0.18)	0.0096 (0.0026)	132 (9)	3 (1)	N/A	N/A	N/A	12 (5)	
F	79.54–82.04	NHmE	Northern Indian Ocean	3.5 (2.1) ^h	0.098 (0.035)	176 (18) ⁱ	15 (7)	0.6 (0.2)	13 (4)	1.6 (0.4)	24 (11)	

^aValues in parenthesis correspond to one standard deviation.

^bFlow regime classification as presented by *Ball et al.* [2003]; NHcT = Northern Hemisphere Continental Tropical; NHcX = Northern Hemisphere Continental Extra-Tropical; NHc = Northern Hemisphere Continental; NHmE = Northern Hemisphere Maritime Equatorial; SHmE = Southern Hemisphere Maritime Equatorial.

^cAir Mass Type classification as presented by *Quinn et al.* [2002].

^dData from NOAA, Pacific Environmental Laboratory (PMEL).

^eCcwK = carbon-containing particles with potassium.

^fAs determined with an Optical Particle Counter (OPC).

^gOnly one data point available for BC.

^hOnly up to DOY 81.98.

ⁱOnly up to DOY 81.35.

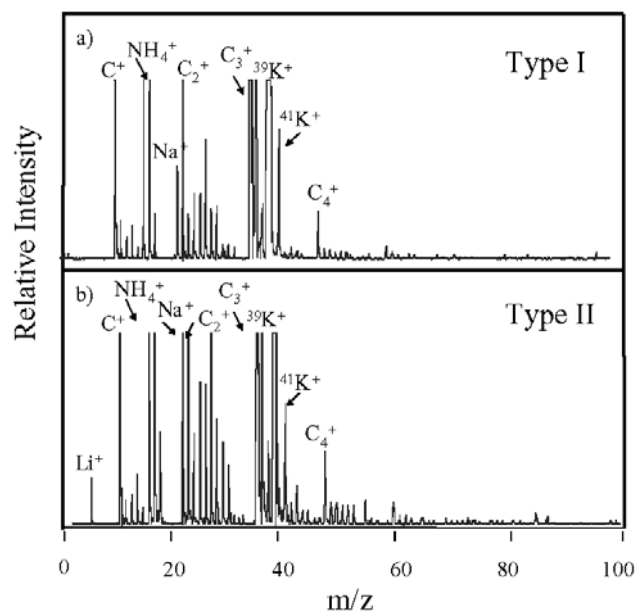


Figure 4. Representative positive ion mass spectra for carbon-containing particles of (a) Type I, and (b) Type II. Peak identifications correspond to the most probable assignments for each particular m/z ratio.

Absorption due to aerosols in different regions sampled during INDOEX is discussed in detail in previous publications [e.g., *Clarke et al.* 2002; *Neusüß et al.* 2002a; *Quinn et al.* 2002].

3.3. Further Classification of Carbon-Containing Particles With Potassium

3.3.1. Carbon-Containing Particles With K⁺ and Lithium

[21] ATOFMS single particle analysis allows for the identification of specific chemical species and combinations of species present in detected particles. In the case of carbon-containing particles with potassium, the presence of certain species can be used as an indication of the original source of the detected particles. From the characteristic mass spectra obtained for carbon-containing particles with K⁺, two major subclasses are identified, and their contributions to the aerosol chemical composition are evaluated. The main characteristics of the two subclasses are shown in Figure 4. For comparison purposes, only positive ion mass spectra of the different particle types up to m/z 100 are presented in Figure 4 since the presence of specific ion clusters in the positive ion mass spectra are used for the sub-classification. In most cases, the mass spectra were very reproducible (i.e., the major ion peaks were almost identical), indicating that the detected particles had originated from the same sources, or very similar sources in different locations, and/or that these particles had undergone similar aging processes. The positive ion mass spectrum presented in Figure 4a was obtained for a carbon-containing particle with K⁺ denoted as Type I. The presence of K⁺ is identified by peaks at m/z 39 and 41 (³⁹K⁺ and ⁴¹K⁺). Also a peak at m/z 18, due to NH₄⁺, appears in the respective positive ion mass spectrum. High concentrations of ammonium have been indicated for aerosol produced from biomass/biofuel

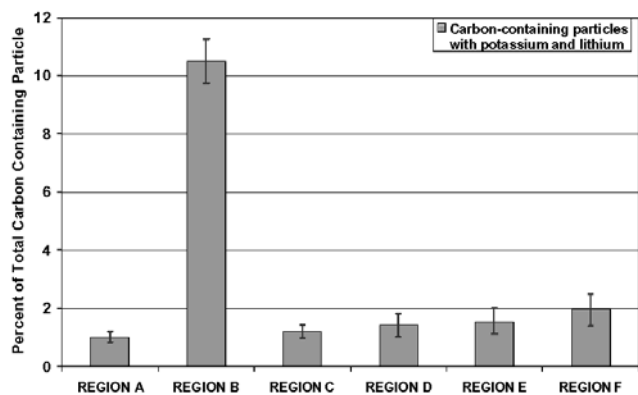


Figure 5. Contribution from carbon-containing particles with potassium and lithium (Type II) to the total number of carbon-containing particles in different regions sampled during INDOEX.

burning [e.g., *Andreae and Crutzen*, 1997]. Peaks at m/z 12, 24, 36, and 48, assigned to C^+ , $(C_2)^+$, $(C_3)^+$, and $(C_4)^+$, respectively, occur as well. In Figure 4b, a typical positive ion mass spectrum for a carbon-containing particle with K^+ of Type II is presented. The main difference with respect to particles of Type I is the presence of lithium (Li^+) at m/z 7 (and a peak due to sodium, Na^+ at m/z 23, with much higher relative intensity).

[22] The presence of lithium in carbonaceous particles could be an indicator of coal combustion. In combustion characterization experiments, lithium was almost never found in the single particle mass spectra of particles produced from biomass/biofuel burning (<0.3%) but it was commonly found in particles produced by coal combustion processes (D. T. Suess et al., manuscript in preparation). The characterization studies described by Suess et al. included several biomass/biofuel and coal sources relevant to the INDOEX study, which were analyzed by ATOFMS single particle analysis as well as by impactor bulk chemical analysis, therefore providing consistent data sets for comparison with the results obtained during the field campaign. Some of the biomass/biofuel sources investigated (of Bangladesh origin) included synthetic logs, dried coconut tree leaves, dried rice straw, and dried cow dung. Coal products studied included chunk coal from Bangladesh, China, India, and USA. It is important to mention that the studied chunk coals were ignited in a brick kiln, therefore producing combustion characteristics close to those commonly encountered in small-scale industrial processes and/or domestic use in India. As indicated by *Reddy and Venkataraman* [2001a], domestic coal combustion processes result in higher particle emissions than industrial ones, due to the lower temperatures used during combustion. Lithium can also be found in dust particles; however, the chemical characteristics of the dust particles are quite different from those arising from fossil fuel combustion sources (see, e.g., *Guazzotti et al.*, 2001; K. R. Coffee et al., manuscript in preparation).

[23] Figure 5 shows the relative contribution of carbon-containing particles with K^+ and Li^+ (Type II) to the total carbon-containing particles. An increase in the contribution of Type II particles was observed for the period DOY

68.08–69.85 (Region B) along with a decrease in the contribution from particles of Type I. As mentioned, during this time period, the sampled air mass had an influence from the Arabian Peninsula. During this time, not only did the overall number concentration of carbon-containing particles with K^+ decrease, but a change in the chemical composition of observed particles occurred as well. Also, low values for the mass concentrations of submicrometer nss K^+ and gas-phase mixing ratios of acetonitrile are observed in this region.

3.3.2. Carbon-Containing Particles Without Potassium

[24] Not all submicrometer carbonaceous particles identified with the ATOFMS contain detectable amounts of potassium [*Guazzotti et al.*, 2001]. The detection limit for potassium in a single particle by ATOFMS is approximately 3×10^{-18} g, this value being one of the lowest determined for several elements [*Silva and Prather*, 1997; *Gross et al.*, 2000]. The relative contribution of carbon-containing particles with no detectable potassium to the total number of carbon-containing particles as observed in different regions is shown in Figure 6. Average contributions are in the range between 19 (± 6)% and 48 (± 18)%. These carbonaceous particles probably derived from the combustion of fossil fuels that contain little or no potassium, such as diesel. In Region B (Arabian influence), the contribution from carbonaceous particles with no detectable potassium (to the total number of carbon-containing particles) is higher than for the other regions. As mentioned above, this could be indicative of a change in the contribution from fossil fuel combustion emissions.

3.4. Single Particle Source Apportionment Estimates for the Contributions From Fossil Fuel Combustion and Biomass/Biofuel Burning to the Total Carbonaceous Aerosol

[25] Taking into consideration the results presented here, an attempt is made to estimate the relative contributions to the carbonaceous aerosol from particles emitted from biomass/biofuel burning with respect to those emitted from fossil fuel combustion. In order to estimate the contribution from particles emitted from biomass/biofuel burning, the

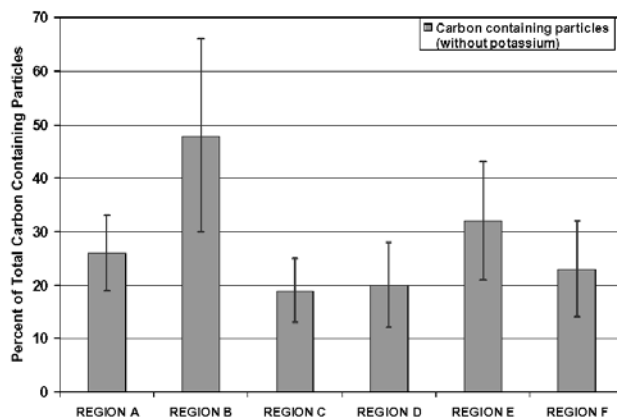


Figure 6. Contribution from carbon-containing particles (with no detectable amount of potassium) to the total number of carbon-containing particles in different regions sampled during INDOEX.

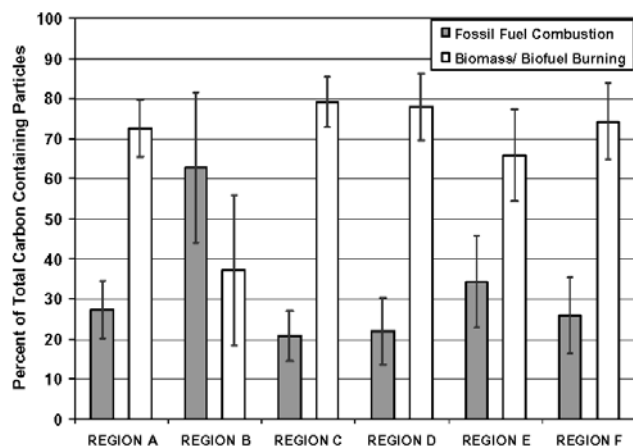


Figure 7. Single particle estimates of relative contributions from biomass/biofuel burning and fossil fuel combustion to the carbonaceous aerosol chemical composition in different regions. The contributions are evaluated as percentage of total carbon-containing particles with aerodynamic diameters between 0.3 and 1.0 μm .

proportion of carbon-containing particles with potassium and lithium (coal) is subtracted from the corresponding contribution from total carbon-containing particles with potassium. The relative contribution from particles emitted from fossil fuel sources is defined as the sum of the average contributions from carbon-containing particles with no detectable potassium (vehicular emissions and/or coal) and those from carbon-containing particles with potassium and lithium (coal). In these calculations, it is assumed that (1) all detected carbon-containing particles with potassium and lithium originate from coal combustion; (2) all carbon-containing particles with no detectable amount of potassium originate from vehicular emissions or other fossil fuel combustion sources that do not produce detectable amounts of potassium (e.g., particles emitted from coal combustion sources that do not contain potassium); and (3) all carbon-containing particles with potassium that do not contain lithium originate from biomass/biofuel burning sources.

[26] The estimates of relative contributions from particles emitted from biomass/biofuel burning and fossil fuel combustion are presented in Figure 7. A substantial change is observed in Region B (Arabian Influence) where the relative contribution of particles emitted from fossil fuel combustion is the highest observed during leg 2, with an average value of 63 (± 19)%. This is in agreement with previously discussed results (section 3.2), where the dominance of fossil fuel has been indicated for that region. For the other regions (A, C–F), the contribution of particles emitted from fossil fuel combustion sources varied between 20 and 34%, with an average value of 26 (± 9)%. For these regions, the estimated average contribution to the total carbonaceous particles from particles emitted from biomass/biofuel sources varied between 73 to 79%, with an evaluated average of 74 (± 9)%.

[27] Reddy and Venkataraman [2001b] have indicated that for the INDOEX period (1998–1999), biomass/biofuel combustion was the major source of carbonaceous aerosols, based on an aerosol emission inventory for India for 1996–

1997. They have estimated that biomass/biofuel burning accounts for 71% of the black carbon emissions and 76% of the organic matter emissions. These estimates for biomass/biofuel contributions are higher than those previously reported for 1990 [Reddy and Venkataraman, 2000]. The analysis presented by Dickerson *et al.* [2002] indicates that 58–88% of the BC arises from biomass/biofuel burning. Our estimates, which correspond to the contributions in number of carbonaceous particles as determined during the field experiment in 1999, are in good agreement with the ones reported by Reddy and Venkataraman [2001b] and Dickerson *et al.* [2002]. From results obtained during three INDOEX research flights, Novakov *et al.* [2000] have estimated the contribution (in mass) of fossil fuel combustion to the carbonaceous aerosol to be approximately 80% using measured BC/TC ratios ($\text{TC} = \text{OC} + \text{BC}$) for their estimations. In our case, the contributions from different particle classes (with different chemical characteristics) to the carbonaceous aerosol chemical composition are considered in the evaluation. The difference in results could be due to changes in the sampled air masses as well as in the actual sampling platform locations and times [Clarke *et al.*, 2002]. As mentioned, the results presented by Novakov *et al.* [2000] were derived from measurements on the C-130 aircraft, whereas the results presented here were obtained on board the R/V Ronald H. Brown. Variability in air masses transport (e.g., long-range transport at high altitudes) and aerosol vertical structure could explain the different estimates. During the INDOEX sampling period, multiple particle layers of variable height and extension have been determined by a six-wavelength lidar [Müller *et al.*, 2001a], showing vertical variability in aerosol properties [Müller *et al.*, 2001a, 2001b]. Measurements by a micro-pulse lidar system have shown that, during leg 2 of the INDOEX cruise, the marine boundary layer (MBL) was usually located below 1000 m with an aerosol layer aloft [Welton *et al.*, 2002]. Therefore the presence of a distinct aerosol layer above the MBL, with different chemical characteristics, could be expected. Also, it has been indicated that during INDOEX, the biomass/biofuel burning influence could have been stronger in the marine boundary layer than in the free troposphere [Reiner *et al.*, 2001], due to differences in the dominant aerosol sources near the surface and at higher altitudes [Rasch *et al.*, 2001]. Meteorological conditions experienced during INDOEX-IFP can help explain the difference in outflow characteristics between the lower troposphere and the layers above the marine boundary layer [Verver *et al.*, 2001]. Also, temporal variations in the biomass/biofuel and fossil fuel contributions to BC have been reported for a surface site in Goa, India [Alfaro *et al.*, 2002]. Based on measured nss K^+ and BC concentration values, and assuming a nss K^+ /BC ratio of 0.52 for biomass/biofuel burning, Alfaro *et al.* [2002] estimated an increased biomass/biofuel influence in the surface site after 10 March 1999 (e.g., as much as 70% of the BC was estimated to arise from biomass/biofuel burning around 23 March versus only 30% for early March 1999).

[28] The calculated contributions of carbonaceous particles from biomass/biofuel burning should be considered as upper estimates, in particular for Region B. There is a possibility that the contributions from carbon-containing particles with K^+ that do not contain Li^+ , arising from local

coal sources, are higher than those evaluated from source characterization studies (D. T. Suess, manuscript in preparation). Also, it could be possible that the ATOFMS technique was unable to detect the presence of Li^+ in some carbon-containing particles with K^+ that contained Li^+ in trace amounts below the detection threshold. The presence of specific markers in the mass spectra of individual particles, such as Li^+ , can be used to refine the estimates, but further characterization studies of single particles produced from combustion processes are necessary for proper assessment. The results presented here for the assignment of possible particle sources from characterization studies represent a first step in the ultimate goal of using single particle signatures for source apportionment. The high correlation found for the number concentration of submicrometer carbon-containing particles with K^+ and the mixing ratio of acetonitrile also indicates that the majority of the carbon-containing particles with K^+ most likely arise from biomass/biofuel burning. Results from other measurements (e.g., trace gases, nonmethane hydrocarbons, CO, CO isotopic ratios [Mühle *et al.*, 2002; Wisthaler *et al.*, 2002]) and source analysis (e.g., source analysis for CO [de Laat *et al.*, 2001]) further support the conclusions presented for leg 2 of the INDOEX cruise.

3.5. Ratios Between Chemical Species in Different Regions

[29] Ratios between different chemical species, for the regions described in the text, are evaluated and presented in this section. Their values are discussed as indications of probable sources (i.e., biomass/biofuel burning and fossil fuel combustion) and compared, when appropriate, with results presented in previous sections.

3.5.1. Nss K^+/BC Ratio

[30] The average submicrometer nss K^+/BC ratios are evaluated for the different regimes from results of submicrometer mass concentration of BC and nss K^+ , as described in sections 2.1 and 2.2 respectively. For the time period DOY 65.07–67.54 (Region A) the average value is determined to be 0.4, whereas for the time period DOY 68.08–69.85 (Region B), the nss K^+/BC ratio has an average value of 0.18. Higher nss K^+/BC ratios in the range between 0.5 and 0.62 are obtained for the remaining regions (Table 1). The relatively high nss K^+/BC ratios indicate that the sampled air masses were probably impacted by biomass/biofuel burning. Reported values for K^+/BC ratios obtained from biomass/biofuel burning are usually in the range between 0.2 and 1.1 depending on the type of fire, the sampled region, and the size of the particles considered for the evaluation [e.g., Andreae, 1983; Ferek *et al.*, 1998; Maenhaut *et al.*, 1996; Reid *et al.*, 1998; Yamasoe *et al.*, 2000; Andreae and Merlet, 2001]. In urban areas, the encountered nss K^+/BC ratios are low (0.025 to 0.09 in the US) [Stevens *et al.*, 1980; Andreae, 1983]. For urban, industrial, and rural areas in Pakistan, Smith *et al.* [1996] have reported K^+/BC ratios of 0.23 for particles with diameters smaller than 10 μm . It has been previously reported that fossil fuel combustion generates little potassium [Andreae, 1983], with K^+/BC ratios for fuel oil combustion being as low as 10^{-5} [Winchester and Nifong, 1971]. Diesel and gasoline engines also produce only small amounts of K^+ [Andreae, 1983]. The low submicrometer nss K^+/BC ratio (0.18)

found in the Arabian air mass (Region B) could be indicative of an increase in the contribution from fossil fuel combustion. A decrease in the relative NH_4^+ concentration has been reported as indicative of a decrease in the relative contribution of particles from biomass/biofuel burning in this region [Ball *et al.*, 2003]. The contribution to BC from biomass/biofuel burning can be estimated using measured nss K^+ and BC values and a typical nss K^+/BC ratio value of 0.52 (± 0.11) for biomass/biofuel burning (at the source) [Cachier *et al.*, 1991; Ferek *et al.*, 1998], in a similar manner to that carried out by Alfaro *et al.* [2002] (i.e., contribution to BC from biomass/biofuel = $100 * ((\text{nss } \text{K}^+ / 0.52) / \text{BC})$). Results from this evaluation yield biomass/biofuel burning contributions to BC of 77% for Region A, 35% for Region B, and 96% for Region C. These values, as well as the corresponding nss K^+/BC ratios, are consistent with the estimates for the contributions from biomass/biofuel burning presented in section 3.4.

3.5.2. Acetonitrile/CO Ratio

[31] As mentioned, acetonitrile is a unique, long-lived tracer for biomass/biofuel burning [e.g., Lobert *et al.*, 1990; Holzinger *et al.*, 1999; Bange and Williams, 2000]. Industrial emissions and fossil fuel combustion are only minor sources of acetonitrile [e.g., Arijs and Brasseur, 1986; Holzinger *et al.*, 2001]. CO is a general marker for incomplete combustion including fossil fuel combustion and biomass/biofuel burning. The evaluation of the acetonitrile/CO enhancement ratio ($\Delta\text{CH}_3\text{CN}/\Delta\text{CO}$) for different air masses encountered during leg 2 of the INDOEX cruise is presented in detail by Wisthaler *et al.* [2002]. Since both trace gases are relatively long-lived, the observed $\Delta\text{CH}_3\text{CN}/\Delta\text{CO}$ enhancement ratio is expected to reflect the source characteristic emission ratio. In air masses from Western India (part of Regions A and C), a $\Delta\text{CH}_3\text{CN}/\Delta\text{CO}$ enhancement ratio of 0.0024 was observed. Laboratory studies of controlled biomass fires covering a large variety of different types of biofuel [Lobert *et al.*, 1991] yielded a mean primary molar emission ratio $\Delta\text{CH}_3\text{CN}/\Delta\text{CO}$ of 0.0025. The strong correlation between CO and acetonitrile ($R^2 = 0.87$) and the similarity of enhancement ratio to the primary emission ratio observed by Lobert *et al.* [1991] indicate that biomass/biofuel burning most likely dominated CO emissions in these regions, which is in agreement with results presented in section 3.4. In the Arabian air mass (Region B), acetonitrile mixing ratios decreased to southern hemispheric background values (see Figure 3) and were not correlated with increasing CO levels [Stehr *et al.*, 2002]. These findings suggest that fossil fuel combustion was the primary source of CO in the Arabian air parcels. From results of single particle apportionment, high contributions from particles emitted from fossil fuel combustion were observed in this region as well (section 3.4).

3.5.3. BC/OC Ratio

[32] As shown in Table 1, high BC/OC ratios for submicrometer particles, in the range between 1.55 and 1.61, were found in all regions with exception of Region B (0.22). These ratios are higher than normally expected solely from biomass/biofuel burning or fossil fuel emissions. For example, from the $\text{PM}_{2.5}$ emission inventory for India [1990] provided by Reddy and Venkataraman [2000], a BC/OC ratio of 0.18–0.27 for fossil fuels, and 0.08–0.22

for biomass/biofuel burning can be derived. From the data compiled by *Andreae and Merlet* [2001] BC/OC ratios of 0.07–0.3 can be determined for various types biomass/biofuel burning. It has been suggested that the high BC/OC ratio observed during INDOEX could mostly be due to emissions of black carbon from fossil fuel combustion processes [*Novakov et al.*, 2000]. High BC emissions are expected for emissions from diesel engines [*Kleeman et al.*, 2000] and certain coal combustion processes (D. T. Suess et al., manuscript in preparation). Some investigators have indicated that known emission factors for fossil fuel cannot account for the high BC concentration values encountered in the region [*Dickerson et al.*, 2002]. In India, biomass/biofuel combustion is considered a major source for carbonaceous aerosol, accounting for 71% of the total BC emissions [*Reddy and Venkataraman*, 2001b]. It is reasonable to expect a substantial amount of BC to originate from biomass/biofuel burning since a positive correlation between BC and CO has been observed in South Asia [*Dickerson et al.*, 2002], and source analysis of CO pollution has found biofuel and agricultural waste burning to be major sources of CO in the region [*de Laat et al.*, 2001]. As previously mentioned, due to the technique employed, the BC concentration values presented here are considered upper limits (see section 2.2) [*Chow et al.*, 2001].

3.5.4. Nss SO_4^{2-} /BC Ratio

[33] The ratios between submicrometer nss sulfate and BC (nss SO_4^{2-} /BC) are evaluated for the different regimes, and the results are summarized in Table 1. The large average values obtained for this ratio for all regions are indicative of the importance of direct emissions and aged particles. Generally, nss SO_4^{2-} is used as tracer for fossil fuel combustion, since only small emissions of sulfate are normally reported for biomass/biofuel burning [e.g., *Crutzen and Andreae*, 1990; *Thornton et al.*, 1999]. Based on the sulfate mass content, a substantial fraction of the total (not only carbonaceous) aerosol mass sampled during INDOEX has been reported to be due to fossil fuel combustion [*Reiner et al.*, 2001; *Lelieveld et al.*, 2001]. However, differences in the estimates of sulfur emissions due to biofuel sources in India are substantial, in particular for cattle dung-cake which produces SO_2 emissions higher than other biofuel sources [*Arndt et al.*, 1997; *Smith et al.*, 2000; *Reddy and Venkataraman*, 2001b]. Also, it has been indicated that biofuel burning can be the dominant contributor to regional SO_2 emissions in a number of developing countries [*Streets and Waldhoff*, 1999]. Sulfur emissions from shipping vessels have been indicated as possible important contributors to SO_2 emissions as well [*Streets et al.*, 2000; *Mayol-Bracero et al.*, 2002]. This could also account for the higher nss SO_4^{2-} /BC ratios determined from the samples collected aboard the R/V Ronald H. Brown when compared with those from the NCAR C-130 aircraft (e.g., ratios between 1.3 and 2.8 have been reported for different flights) [*Novakov et al.*, 2000; *Clarke et al.*, 2002; *Mayol-Bracero et al.*, 2002].

4. Conclusions

[34] Results obtained by traditional standardized aerosol particle chemical analysis, real-time single-particle analysis,

and fast-response gas-phase PTR-MS reflect the impact of different meteorological regimes and air masses encountered during leg 2 of the R/V Ronald H. Brown INDOEX cruise. Low overall concentrations are found in the southernmost regions sampled where the air masses did not have any recent land influence. High values for concentration of submicrometer nss K^+ , carbon-containing particles with K^+ , acetonitrile mixing ratio, and submicrometer nss K^+ /EC ratios are observed in air masses advected from India. Results from an extended set of measurements imply a high contribution to carbonaceous aerosols from biomass/biofuel burning (accounting for approximately 75% of the carbon-containing particles), even in areas far from sources, showing the possibility of long-range transport (up to 7 days, as indicated by back trajectory analysis).

[35] In air parcels from the Arabian Peninsula, the overall number concentration of carbon-containing particles with K^+ , the submicrometer nss K^+ mass concentration, and the acetonitrile mixing ratio decreased resulting in a smaller nss K^+ /EC and acetonitrile/CO ratio. These findings indicate a reduced biomass/biofuel burning impact and a higher contribution from fossil fuel combustion. A higher relative contribution from carbon-containing particles with K^+ and Li^+ indicate a higher relative contribution of carbonaceous particles from coal combustion derived particles, since carbon-containing particles with potassium and lithium have been observed in related source characterization studies. Also, carbon-containing particles with no detectable amount of potassium were enhanced in this region, indicating a stronger impact from fossil fuel combustion. Future studies involving further chemical characterization from different sources will be essential for minimizing some of the uncertainties, allowing for proper assessments of Asia's pollution impact on regional and global scales.

[36] **Acknowledgments.** This work was supported in part by: the National Science Foundation via the Center for Clouds Chemistry and Climate (C^4) at the Scripps Institution of Oceanography under Grants ATM-9612887 and ATM-9405024; the Aerosol Project of the NOAA Climate and Global Change Program; the Global Aerosol Climatology Project of the NASA Earth System Science Program; and the Bundesministerium für Bildung, Wissenschaft, Forschung und Technik (BMBF) under contract LA-9830/0. We thank the captain and crew of the NOAA R/V Ronald H. Brown for their help and support.

References

- Alfaro, S. C., A. Gaudichet, J. L. Rajot, L. Gomes, M. Maille, and H. Cachier, Variability of aerosol size-resolved composition at an Indian coastal site during INDOEX intensive field phase, *J. Geophys. Res.*, 108(D8), 4235, doi:10.1029/2002JD002645, 2002.
- Allen, J. O., D. P. Fergenson, E. E. Gard, L. S. Hughes, B. D. Morrical, M. J. Kleeman, D. S. Gross, M. E. Galli, K. A. Prather, and G. R. Cass, Particle detection efficiencies of aerosol time of flight mass spectrometers under ambient sampling conditions, *Environ. Sci. Technol.*, 34(1), 211–217, 2000.
- Anderson, T. L., D. S. Covert, J. D. Wheeler, J. M. Harris, K. D. Perry, B. E. Trost, D. J. Jaffe, and J. A. Ogren, Aerosol backscatter fraction and single scattering albedo: Measured values and uncertainties at a coastal station in the Pacific Northwest, *J. Geophys. Res.*, 104(D21), 26,793–26,807, 1999.
- Andreae, M. O., Soot carbon and excess fine potassium: Long-range transport of combustion-derived aerosols, *Science*, 220, 1148–1151, 1983.
- Andreae, M. O., Biomass burning: Its history, use, and distribution and its impact on environmental quality and global climate, in *Global Biomass Burning: Atmospheric, Climatic and Biospheric Implications*, edited by J. S. Levine, pp. 3–21, MIT Press, Cambridge, Mass., 1991.

- Andreae, M. O., and P. J. Crutzen, Atmospheric aerosols: Biogeochemical sources and role in atmospheric chemistry, *Science*, 276(5315), 1052–1058, 1997.
- Andreae, M. O., and P. Merlet, Emissions of trace gases and aerosols from biomass burning, *Global Biogeochem. Cycles*, 15, 955–966, 2001.
- Andreae, M. O., E. Atlas, H. Cachier, W. R. Cofer III, G. W. Harris, G. Helas, R. Kopppmann, J.-P. Lacaux, and D. E. Ward, Trace gas and aerosol emissions from savanna fires, in *Biomass Burning and Global Change*, vol. 1, edited by J. S. Levine, pp. 278–295, MIT Press, Cambridge, Mass., 1996.
- Arijs, E., and G. Brasseur, Acetonitrile in the stratosphere and implication for positive ion composition, *J. Geophys. Res.*, 91, 4003–4016, 1986.
- Arndt, R. L., G. R. Carmichael, D. G. Streets, and N. Bhatti, Sulfur dioxide emissions and sectorial contributions to sulfur deposition in Asia, *Atmos. Environ.*, 31, 1553–1572, 1997.
- Ball, W. P., R. R. Dickerson, B. G. Doddridge, J. W. Stehr, T. L. Miller, D. L. Savoie, and T. P. Carsey, Bulk and size-segregated aerosol composition observed during INDOEX 1999: Overview of meteorology and continental impacts, *J. Geophys. Res.*, 108(D10), 8001, doi:10.1029/2002JD002467, 2003.
- Bange, H. W., and J. Williams, New Directions: Acetonitrile in atmospheric and biogeochemical cycles, *Atmos. Environ.*, 34(28), 4959–4960, 2000.
- Bates, T. S., D. J. Coffman, D. S. Covert, and P. K. Quinn, Regional marine boundary layer aerosol size distributions in the Indian, Atlantic, and Pacific Oceans: A comparison of INDOEX measurements with ACE-1, ACE-2, and Aerosols99, *J. Geophys. Res.*, 107(D9), 8026, doi:10.1029/2001JD001174, 2002.
- Berner, A., C. Lurzer, F. Pohl, O. Preining, and P. Wagner, The size distribution of the urban aerosol in Vienna, *Sci. Total Environ.*, 13, 245–261, 1979.
- Bond, T. C., T. L. Anderson, and D. Campbell, Calibration and intercomparison of filter-based measurements of visible light absorption by aerosols, *Aerosol Sci. Technol.*, 30(6), 82–600, 1999.
- Cachier, H., and J. Ducret, Influence of biomass burning on equatorial African rains, *Nature*, 352(6332), 228–230, 1991.
- Cachier, H., M. P. Bremond, and P. Buat-Menard, Carbonaceous aerosols from different tropical biomass burning sources, *Nature*, 340(6232), 371–373, 1989.
- Cachier, H., J. Ducret, M. P. Bremond, A. Gaudichet, V. Yoboue, J. P. Lacaux, and J. Baudet, in *Global Biomass Burning: Atmospheric, Climatic, and Biospheric Implications*, edited by J. S. Levine, pp. 174–180, MIT Press, Cambridge, Mass., 1991.
- Cadle, S. H., and P. A. Mulawa, Atmospheric carbonaceous species measurement methods comparison study: General Motors results, *Aerosol Sci. Technol.*, 12, 128–141, 1990.
- Charlson, R. J., J. Langner, H. Rodhe, C. B. Leovy, and S. G. Warren, Perturbation of the northern hemisphere radiative balance by backscattering from anthropogenic sulfate aerosols, *Tellus, Ser. A*, 43(4), 152–163, 1991.
- Chow, J. C., J. G. Watson, D. Crow, D. H. Lowenthal, and T. Merrifield, Comparison of IMPROVE and NIOSH carbon measurements, *Aerosol Sci. Technol.*, 34, 23–34, 2001.
- Clarke, A., et al., INDOEX aerosol: A comparison and summary of microphysical, chemical and optical properties observed from land, ship and aircraft, *J. Geophys. Res.*, 107(D19), 8033, doi:10.1029/2001JD000572, 2002.
- Coakley, J. A., and R. D. Cess, Response of the NCAR community climate model to the radiative forcing by the naturally-occurring tropospheric aerosol, *J. Atmos. Sci.*, 42, 1677–1692, 1985.
- Cooke, W. F., and J. J. N. Wilson, A global black carbon aerosol model, *J. Geophys. Res.*, 101(D14), 19,395–19,409, 1996.
- Countes, R. J., Interlaboratory analyses of carbonaceous samples, *Aerosol Sci. Technol.*, 12, 114–121, 1990.
- Crutzen, P. J., and M. O. Andreae, Biomass burning in the tropics: Impact on atmospheric chemistry and biogeochemical cycles, *Science*, 250(4988), 1669–1678, 1990.
- de Laat, A. T. J., J. Lelieveld, G. J. Roelofs, R. R. Dickerson, and J. M. Lobert, Source analysis of carbon monoxide during INDOEX 1999, *J. Geophys. Res.*, 106, 28,481–28,495, 2001.
- Desalmand, F., R. Serpelay, and J. Podzimek, Some specific features of the aerosol particle concentrations during the dry season and during a bush-fire event in West Africa, *Atmos. Environ.*, 19, 1535–1543, 1985.
- Dickerson, R. R., M. O. Andreae, T. Campos, O. L. Mayol-Bracero, C. Neusuess, and D. G. Streets, Analysis of black carbon and carbon monoxide observed over the Indian Ocean: Implications for emissions and photochemistry, *J. Geophys. Res.*, 107(D9), 8017, doi:10.1029/2001JD000501, 2002.
- Draxler, R. R., The accuracy of trajectories during Anatex calculated using dynamic model analyses versus rawinsonde observations, *J. Appl. Meteorol.*, 30(10), 1446–1467, 1991.
- Draxler, R. R., and G. D. Hess, An overview of the Hysplit 4 modeling system for trajectories, dispersion and deposition, *Aust. Meteorol. Mag.*, 47, 295–308, 1998.
- Ferek, R. J., J. S. Reid, P. V. Hobbs, D. R. Blake, and C. Lioussé, Emission factors of hydrocarbons, halocarbons, trace gases and particles from biomass burning in Brazil, *J. Geophys. Res.*, 103(D24), 32,107–32,118, 1998.
- Gard, E., J. E. Mayer, B. D. Morrical, T. Dienes, D. P. Fergenson, and K. A. Prather, Real-time analysis of individual atmospheric aerosol particles: Design and performance of a portable ATOFMS, *Anal. Chem.*, 69(20), 4083–4091, 1997.
- Gaudichet, A., F. Echalar, B. Chatenet, J.P. Quisefit, G. Malingre, H. Cachier, P. Buat-Menard, P. Artaxo, and W. Maenhaut, Trace elements in tropical African Savanna biomass burning aerosols, *J. Atmos. Chem.*, 22(1–2), 19–39, 1995.
- Gross, D. S., M. E. Galli, P. J. Silva, and K. A. Prather, Relative sensitivity factors for alkali metal and ammonium cations in single particle aerosol time-of-flight mass spectra, *Anal. Chem.*, 72(2), 416–422, 2000.
- Guazzotti, S. R., K. R. Coffee, and K. A. Prather, Continuous measurements of size resolved particle chemistry during INDOEX-IPF 99, *J. Geophys. Res.*, 106(22), 28,607–28,627, 2001.
- Hall, D. O., F. Rosilloccale, and J. Woods, Biomass utilization in households and industry: Energy use and development, *Chemosphere*, 29(5), 1099–1119, 1994.
- Hall, D. O., G. W. Bamar, and P. A. Moss, *Biomass for Energy in the Developing Countries*, Pergamon, New York, 1992.
- Hallet, J., J. G. Hudson, and C. F. Rogers, Characterization of combustion aerosols for haze and cloud formation, *Aerosol Sci. Technol.*, 10, 70–83, 1989.
- Hansel, A., A. Jordan, R. Holzinger, P. Prazeller, W. Vogel, and W. Lindinger, Proton transfer reaction mass spectrometry: On-line trace gas analysis at the ppbv level, *Int. J. Mass Spectrom. Ion Processes*, 149/150, 609–619, 1995.
- Haywood, J., and O. Boucher, Estimates of the direct and indirect radiative forcing due to tropospheric aerosols: A review, *Rev. Geophys.*, 38(4), 513–543, 2000.
- Haywood, J. M., and K. P. Shine, Multi-spectral calculations of the direct radiative forcing of tropospheric sulphate and soot aerosols using a column model, *Q. J. R. Meteorol. Soc.*, 123(543), 1907–1930, 1997.
- Haywood, J. M., and K. P. Shine, The effect of anthropogenic sulfate and soot aerosol on the clear sky planetary radiation budget, *Geophys. Res. Lett.*, 22(5), 603–606, 1995.
- Haywood, J. M., D. L. Roberts, A. Slingo, J. M. Edwards, and K. P. Shine, General circulation model calculations of the direct radiative forcing by anthropogenic sulfate and fossil-fuel soot aerosol, *J. Clim.*, 10(7), 1562–1577, 1997.
- Holzinger, R., A. Jordan, A. Hansel, and W. Lindinger, Automobile emissions of acetonitrile: Assessment of its contribution to the global source, *J. Atmos. Chem.*, 38(2), 187–193, 2001.
- Holzinger, R., C. Warneke, A. Hansel, A. Jordan, W. Lindinger, D. H. Scharffe, G. Schade, and P. J. Crutzen, Biomass burning as a source of formaldehyde, acetaldehyde, methanol, acetone, acetonitrile, and hydrogen cyanide, *Geophys. Res. Lett.*, 26(8), 1161–1164, 1999.
- Howell, S., A. A. P. Pszenny, P. Quinn, and B. Huebert, A field intercomparison of three cascade impactors, *Aerosol Sci. Technol.*, 29(6), 475–492, 1998.
- Hughes, L. S., et al., Size and composition distribution of atmospheric particles in southern California, *Environ. Sci. Technol.*, 33(20), 3506–3515, 1999.
- Intergovernmental Panel on Climate Change (IPCC), Climate change, 1995: The science of climate change, Cambridge Univ. Press, New York, 1996.
- Iversen, T., and L. Tarrason, On climatic effects of arctic aerosols, *Inst. Rep. Ser., Report No. 94*, Dep. of Geophysics, Oslo, Norway, 1995.
- Iversen, T., A. Kirkevåg, and O. Seland, Hemispheric modeling of sulphate and black carbon and their direct effects, in *Air Pollution Modeling and its Applications*, XII, edited by C. Gryning, pp. 477–480, Plenum Press, New York, 1998.
- Jacobson, M. Z., Strong radiative heating due to the mixing state of black carbon in atmospheric aerosols, *Nature*, 409(6821), 695–697, 2001.
- Kleeman, M. J., J. J. Schauer, and G. R. Cass, Size and composition distribution of fine particulate matter emitted from motor vehicles, *Environ. Sci. Technol.*, 34(7), 1132–1142, 2000.
- Kuhlbusch, T. A. J., M. O. Andreae, H. Cachier, J. G. Goldammer, J. P. Lacaux, R. Shea, and P. J. Crutzen, Black carbon formation by Savanna fires: Measurements and implications for the global carbon cycle, *J. Geophys. Res.*, 101(D19), 23,651–23,665, 1996.
- Lelieveld, J., et al., The Indian Ocean experiment: Widespread air pollution from South and Southeast Asia, *Science*, 291, 1031–1036, 2001.

- Lindinger, W., A. Hansel, and A. Jordan, Proton-transfer-reaction mass spectrometry (PTR-MS): On-line monitoring of volatile organic compounds at pptv levels, *Chem. Soc. Rev.*, 27, 347–354, 1998.
- Liu, X. D., P. Van Espen, F. Adams, J. Cafmeyer, and W. Maenhaut, Biomass burning in southern Africa: Individual particle characterization of atmospheric aerosols and savanna fire samples, *J. Atmos. Chem.*, 36, 135–155, 2000.
- Lobert, J. M., D. H. Scharffe, W. M. Hao, and P. J. Crutzen, Importance of biomass burning in the atmospheric budgets of nitrogen-containing gases, *Nature*, 346(6284), 552–554, 1990.
- Lobert, J. M., et al., Experimental evaluation of biomass burning emissions: Nitrogen and carbon containing compounds, in *Global Biomass Burning: Atmospheric, Climatic, and Biospheric Implications*, edited by J. S. Levine, pp. 289–303, MIT Press, Cambridge, Mass., 1991.
- Maenhaut, W., I. Salma, J. Cafmeyer, H. J. Annegam, and M. O. Andreae, Regional atmospheric aerosol composition and sources in the eastern Transvaal, South Africa, and impact of biomass burning, *J. Geophys. Res.*, 101(D19), 23,631–23,650, 1996.
- Mayol-Bracero, O. L., R. Gabriel, M. O. Andreae, T. W. Kirchstetter, T. Novakov, and D. G. Streets, Carbonaceous aerosols over the Indian Ocean during INDOEX: Chemical characterization, optical properties, and probable sources, *J. Geophys. Res.*, 107(D19), 8030, doi:10.1029/2000JD000039, 2002.
- Mitra, A. P., INDOEX (India): Introductory note, *Curr. Sci.*, 76(7), 886–889, 1999.
- Mühle, J., A. Zahn, C. A. M. Brenninkmeijer, V. Gros, and P. J. Crutzen, Air mass classification during INDOEX R/V Ronald Brown cruise using measurements of nonmethane hydrocarbons, CH₄, CO₂, CO, ¹⁴CO, and δ¹⁸O (CO), *J. Geophys. Res.*, 107(D19), 8021, doi:10.1029/2001JD000730, 2002.
- Müller, D., K. Franke, F. Wagner, D. Althausen, A. Ansmann, and J. Heintzenberg, Vertical profiling of optical particle properties over the tropical Indian Ocean with six-wavelength lidar: 1. Seasonal cycle, *J. Geophys. Res.*, 106, 28,567–28,575, 2001a.
- Müller, D., K. Franke, F. Wagner, D. Althausen, A. Ansmann, and J. Heintzenberg, Vertical profiling of optical particle properties over the tropical Indian Ocean with six-wavelength lidar: 2. Case studies, *J. Geophys. Res.*, 106, 28,577–28,595, 2001b.
- Neusüß, C., T. Gnauk, A. Plewka, H. Herrmann, and P. K. Quinn, Carbonaceous aerosol over the Indian Ocean: OC/EC fractions and selected specifications from size-segregated onboard samples, *J. Geophys. Res.*, 107(D19), 8031, doi:10.1029/2001JD000327, 2002a.
- Neusüß, C., H. Wex, W. Birmili, A. Wiedensohler, C. Koziar, B. Busch, E. Brüggemann, and T. Gnauk, Characterization and parameterization of atmospheric particle number-, mass-, and chemical-size distributions in central Europe during LACE 98 and MINT, *J. Geophys. Res.*, 107(D21), 8127, doi:10.1029/2001JD000514, 2002b.
- Noble, C. A., and K. A. Prather, Real-time measurement of correlated size and composition profiles of individual atmospheric aerosol particles, *Environ. Sci. Technol.*, 30, 2667–2680, 1996.
- Novakov, T., M. O. Andreae, R. Gabriel, T. W. Kirchstetter, O. L. Mayol-Bracero, and V. Ramanathan, Origin of carbonaceous aerosols over the tropical Indian Ocean: Biomass burning or fossil fuels?, *Geophys. Res. Lett.*, 27(24), 4061–4064, 2000.
- Parsons, R. L., and R. R. Dickerson, NOAA ship Ronald H. Brown: Study global climate variability, *Sea Technol.*, 40(6), 39–45, 1999.
- Penner, J. E., R. E. Dickinson, and C. A. O'Neill, Effects of aerosol from biomass burning on the global radiation budget, *Science*, 256(5062), 1432–1434, 1992.
- Penner, J. E., H. Eddleman, and T. Novakov, Towards the development of a global inventory for black carbon emissions, *Atmos. Environ., Part A*, 27(8), 1277–1295, 1993.
- Podgorny, I. A., W. Conant, V. Ramanathan, and S. K. Satheesh, Aerosol modulation of atmospheric and surface solar heating over the tropical Indian Ocean, *Tellus, Ser. B*, 52(3), 947–958, 2000.
- Prather, K. A., T. Nordmeyer, and K. Salt, Real-time characterization of individual aerosol particles using time-of-flight mass spectrometry, *Anal. Chem.*, 66(9), 1403–1407, 1994.
- Pszenny, A. A. P., Particle size distributions of methanesulfonate in the tropical Pacific marine boundary layer, *J. Atmos. Chem.*, 14(1–4), 273–284, 1992.
- Quinn, P. K., D. J. Coffmann, V. N. Kapustin, T. S. Bates, and D. S. Covert, Aerosol optical properties in the marine boundary layer during the First Aerosol Characterization Experiment (ACE 1) and the underlying chemical and physical aerosol properties, *J. Geophys. Res.*, 103(D13), 16,547–16,563, 1998.
- Quinn, P. K., D. J. Coffmann, T. S. Bates, T. L. Miller, J. E. Johnson, K. Voss, E. J. Welton, C. Neusüß, P. Miller, and J. Sheridan, Aerosol optical properties during INDOEX 999: Means, variability, and controlling factors, *J. Geophys. Res.*, 107(D9), 8020, doi:10.1029/2000JD000037, 2002.
- Ramanathan, V., et al., Indian Ocean Experiment (INDOEX) White Paper, C⁴, Scripps Inst. of Oceanogr., La Jolla, Calif., 1995.
- Ramanathan, V., et al., Indian Ocean Experiment (INDOEX), A multi-agency proposal for field experiment in the Indian Ocean, C⁴ publ. 162, 83 pp., Scripps Inst. of Oceanogr., La Jolla, Calif., 1996.
- Ramanathan, V., et al., The Indian Ocean Experiment: Widespread haze from south and southeast Asia and its climate forcing, *J. Geophys. Res.*, 106, 28,371–28,398, 2001.
- Rasch, P. J., W. D. Collins, and B. E. Eaton, Understanding the Indian Ocean Experiment (INDOEX) aerosol distributions with an aerosol assimilation, *J. Geophys. Res.*, 106(D7), 7337–7355, 2001.
- Ravindranath, N. H., and D. O. Hall, *Biomass, Energy and Environment: A Developing Country Perspective From India*, Oxford Univ. Press, New York, 1995.
- Reddy, M. S., and C. Venkataraman, Atmospheric optical and radiative effects of anthropogenic aerosol constituents from India, *Atmos. Environ.*, 34(26), 4511–4523, 2000.
- Reddy, M. S., and C. Venkataraman, Inventory of aerosol and sulphur dioxide emissions from India: Part Fossil fuel combustion, I., *Atmos. Environ.*, 36(4), 677–697, 2001a.
- Reddy, M. S., and C. Venkataraman, Inventory of aerosol and sulphur dioxide emissions from India: Part II. Biomass combustion, *Atmos. Environ.*, 36(4), 699–712, 2001b.
- Reid, J. S., P. V. Hobbs, C. Liousse, J. V. Martins, R. E. Weiss, and T. F. Eck, Comparisons of techniques for measuring shortwave absorption and black carbon content of aerosols from biomass burning in Brazil, *J. Geophys. Res.*, 103(D24), 32,031–32,040, 1998.
- Reiner, T., D. Sprung, C. Jost, R. Gabriel, O. L. Mayol-Bracero, M. O. Andreae, T. L. Campos, and R. E. Shetter, Chemical characterization of pollution layers over the tropical Indian Ocean: Signature of emissions from biomass and fossil fuel burning, *J. Geophys. Res.*, 106(D22), 28,497–28,510, 2001.
- Rosenfeld, D., Suppression of rain and snow by urban and industrial air pollution, *Science*, 287(5459), 1793–1796, 2000.
- Ruellan, S., H. Cachier, A. Gaudichet, P. Masclet, and J. P. Lacaux, Airborne aerosols over central Africa during the experiment for regional sources and sinks of oxidants (EXPRESSO), *J. Geophys. Res.*, 104, 30,673–30,690, 1999.
- Satheesh, S. K., V. Ramanathan, L. J. Xu, J. M. Lobert, I. A. Podgorny, J. M. Prospero, B. N. Holben, and N. G. Loeb, A model for the natural and anthropogenic aerosols over the tropical Indian Ocean derived from Indian Ocean Experiment data, *J. Geophys. Res.*, 104(D22), 27,421–27,440, 1999.
- Schmid, H., et al., Results of the “Carbon Conference” international carbon round robin test stage I, *Atmos. Environ.*, 35/12, 2111–2121, 2001.
- Schwartz, S. E., and M. O. Andreae, Uncertainty in climate change caused by aerosols, *Science*, 272(5265), 1121–1122, 1996.
- Schwartz, S. E., The white house effect: Shortwave radiative forcing of climate by anthropogenic aerosols: An overview, *J. Aerosol Sci.*, 27(3), 359–382, 1996.
- Shah, J. J., and J. A. Rau, Carbonaceous species methods comparison study: Interlaboratory round robin interpretation of results, Res. Div., Calif. Air Res. Board, *Final Rep. G2E-0024*, Sacramento, Calif., 1991.
- Silva, P. J., and K. A. Prather, On-line characterization of individual particles from automobile emissions, *Environ. Sci. Technol.*, 31(11), 3074–3080, 1997.
- Silva, P. J., D.-Y. Liu, C. A. Noble, and K. A. Prather, Size and chemical characterization of individual particles resulting from biomass burning of local Southern California species, *Environ. Sci. Technol.*, 33(18), 3068–3076, 1999.
- Smith, D. J. T., R. M. Harrison, L. Luhana, C. A. Pio, L. M. Castro, M. N. Tariq, S. Hayat, and T. Quraishi, Concentrations of particulate airborne polycyclic aromatic hydrocarbons and metals collected in Lahore, Pakistan, *Atmos. Environ.*, 30(23), 4031–4040, 1996.
- Smith, K. R., R. Uma, V. V. N. Kishore, K. Lata, V. Joshi, J. Zhang, R. A. Rasmussen, and M. A. K. Khalil, Greenhouse gases from small-scale combustion devices in developing countries: Phase I Household stoves in India, I., *EPA-600/R-00-052*, Office of Res. and Dev., U.S. Environ. Protect. Agency, Washington, D.C., 2000.
- Sprung, D., C. Jost, T. Reiner, A. Hansel, and A. Wisthaler, Acetone and acetonitrile in the tropical Indian Ocean boundary layer and free troposphere: Aircraft-based intercomparison of AP-CIMS and PTR-MS measurements, *J. Geophys. Res.*, 106, 28,511–28,527, 2001.
- Stehr, J. W., W. P. Ball, R. R. Dickerson, B. G. Doddridge, C. Piety, and J. E. Johnson, Latitudinal gradients in O₃ and CO during INDOEX 1999, *J. Geophys. Res.*, 107(D19), 8016, doi:10.1029/2001JD000446, 2002.
- Stevens, R. K., T. G. Dzubay, R. W. Shaw Jr., W. A. McClenny, C. W. Lewis, and W. E. Wilson, *Science*, 14, 1491, 1980.

- Streets, D. G., and S. T. Waldhoff, Greenhouse-gas emissions from biofuel combustion in Asia, *Energy*, 24, 841–855, 1999.
- Streets, D. G., S. K. Guttikunda, and G. R. Carmichael, The growing contribution of sulfur emissions from ships in Asian waters, 1988–1995, *Atmos. Environ.*, 34, 4425–4439, 2000.
- Thornton, D. C., A. R. Bandy, B. W. Blomquist, A. R. Driedger, and T. P. Wade, Sulfur dioxide contribution over the Pacific Ocean 1991–1996, *J. Geophys. Res.*, 104, 5845–5854, 1999.
- Turpin, B. J., J. J. Huntzicker, and S. V. Hering, Investigation of organic aerosol sampling artifacts in the Los Angeles Basin, *Atmos. Environ.*, 28, 3061–3071, 1994.
- Twomey, S., *Atmospheric Aerosols*, 302 pp., Elsevier Sci., New York, 1977.
- United Nations Environmental Program (UNEP), Environmental impacts of trade liberalization and policies for sustainable management of natural resources: A case study on India's automobile sector, *UNEP/99/2*, 177 pp., United Nations Environ. Programme, Nairobi, 1999.
- United Nations Environmental Program (UNEP), Assessment Report, Asian brown cloud: Climate and other environmental impacts, UNEP and C4, United Nations Environ. Programme, Nairobi, 2002.
- Verver, G. H. L., D. R. Sikka, J. M. Lobert, G. Stossmeister, and M. Zachariasse, Overview of the meteorological conditions and atmospheric transport processes during INDOEX 1999, *J. Geophys. Res.*, 106, 28,399–28,413, 2001.
- Wang, H.-C., and W. John, Characteristics of the Berner impactor for sampling inorganic ions, *Aerosol Sci. Technol.*, 8, 157–172, 1988.
- Welton, E. J., K. J. Voss, P. K. Quinn, P. J. Flatau, K. Markowicz, J. R. Campbell, J. D. Spinhirne, H. R. Gordon, and J. E. Johnson, Measurements of aerosol vertical profiles and optical properties during INDOEX 1999 using micro-pulse lidars, *J. Geophys. Res.*, 107(D9), 8019, doi:10.1029/2000JD000038, 2002.
- Wenzel, R. J., D.-Y. Liu, E. S. Edgerton, and K. A. Prather, Aerosol time-of-flight mass spectrometry during the Atlanta Supersite Experiment: 2. Scaling procedures, *J. Geophys. Res.*, 108(D7), 8427, doi:10.1029/2001JD001563, 2003.
- Winchester, J. W., and G. D. Nifong, Water pollution in Lake Michigan by trace elements from pollution aerosol fallout, *Water Air Soil Pollut.*, 1, 50–64, 1971.
- Wisthaler, A., A. Hansel, P. Crutzen, and R. Dickerson, Organic trace gas measurements by PTR-MS during INDOEX 1999, *J. Geophys. Res.*, 107(D19), 8024, doi:10.1029/2001JD000576, 2002.
- Yamasoe, M. A., A. Paulo, A. H. Miguel, and A. G. Allen, Chemical composition of aerosol particles from different emissions of vegetation fires in the Amazon Basin: Water-soluble species and trace elements, *Atmos. Environ.*, 34, 1641–1653, 2000.
-
- W. P. Ball, Department of Chemistry, University of Maryland, College Park, MD 20742, USA. (ball@metosrv2.umd.edu)
- T. S. Bates and P. K. Quinn, NOAA, Pacific Marine Environmental Laboratory, 7600 Sand Point Way, NE, Seattle, WA 98115, USA. (bates@pmel.noaa.gov; quinn@pmel.noaa.gov)
- K. R. Coffee, Lawrence Livermore National Laboratory, 7000 East Ave L-231, Livermore, CA 94550, USA. (coffee3@llnl.gov)
- P. J. Crutzen, Atmospheric Chemistry Division, Max-Planck Institute for Chemistry, J.J. Becher-weg 27, D-55128 Mainz, Germany. (aira@mpch-mainz.mpg.de)
- R. R. Dickerson, Department of Meteorology and Department of Chemistry, University of Maryland, College Park, MD 20742, USA. (russ@atmos.umd.edu)
- S. A. Guazzotti, Department of Chemistry and Biochemistry, University of California, San Diego, CA 92037, USA. (serad@chem.ucsd.edu)
- A. Hansel and A. Wisthaler, Institut für Ionenphysik, University of Innsbruck, Technikerstrasse 25, A-6020, Innsbruck, Austria. (Armin.Hansel@uibk.ac.at; Armin.Wisthaler@uibk.ac.at)
- C. Neusüß, Bruker Daltonik GmbH, Permoser Str. 15, D-04318 Leipzig, Germany. (cne@bdal.de)
- K. A. Prather, Department of Chemistry and Biochemistry, University of California, San Diego, 9500 Gilman Drive, La Jolla, CA 92093, USA. (kprather@chem.ucsd.edu)
- D. T. Suess, Department of Chemistry, University of California, Riverside, CA 92521, USA. (dtsuess@citrus.ucr.edu)